Journal of Dentistry 91 (2019) 103231

Contents lists available at ScienceDirect

Journal of Dentistry

journal homepage: www.elsevier.com/locate/jdent

Comparison of the use of D-enantiomeric and L-enantiomeric antimicrobial peptides incorporated in a calcium-chelating irrigant against *Enterococcus faecalis* root canal wall biofilms

Wei-hu Ye[a], Lara Yeghiasarian[b], Christopher W. Cutler[b], Brian E. Bergeron[b], Stephanie Sidow[b], Hockin H.K. Xu[c], Li-na Niu[b,d,e,*], Jing-zhi Ma[a,**], Franklin R. Tay[b,*]

[a] Department of Stomatology, Tongji Hospital, Tongji Medical College, Huazhong University of Science and Technology, Wuhan, China
[b] The Dental College of Georgia, Augusta University, Augusta, GA, USA
[c] Department of Advanced Oral Sciences and Therapeutics, University of Maryland School of Dentistry, Baltimore, MD, USA
[d] State Key Laboratory of Military Stomatology & National Clinical Research Center for Oral Diseases & Shaanxi Key Laboratory of Stomatology, Department of Prosthodontics, School of Stomatology, The Fourth Military Medical University, Xi'an, China
[e] The Third Affiliated Hospital of Xinxiang Medical University, Xinxiang, Henan, China

ARTICLE INFO

Keywords:
Antimicrobial peptide
Biofilm
E. faecalis
Irrigant
Root canal

ABSTRACT

Objectives: To compare the anti-biofilm efficacy of two antimicrobial peptides (AMPs), 1018 and DJK-5, in disrupting canal wall biofilms in the isthmus, canal and dentinal tubules of single-rooted maxillary premolars.
Methods: *Enterococcus faecalis* single-species biofilms were formed in-situ in the root canal system of the premolars (n = 91). Confocal laser scanning microscopy, bacterial sampling, colony-forming unit counting, XTT assay, lactate dehydrogenase assay and phenol-sulphuric acid method were used to identify the anti-biofilm efficacy of both AMPs and their influence on bacterial metabolic activity.
Results: Both AMPs disrupted in-situ *E. faecalis* biofilms and altered their metabolic activity. At 20 μg/mL, the D-enantiomeric AMP DJK-5 killed 55.5 %, 57.3 % and 55.8 % of biofilm bacteria in the isthmus, canal and dentinal tubules, respectively, in 1 min. In contrast, the L-enantiomeric AMP 1018 only eradicated 25.6 %, 25.5 % and 27.5 % of biofilm bacteria in the isthmus, canal and dentinal tubules, respectively, within the same time. Anti-biofilm efficacy of the root canal irrigants tested were in the order: 6 % NaOCl > 20 μg/mL DJK-5 > 10 μg/mL DJK-5 > 20 μg/mL 1018 > 10 μg/mL 1018 > 0.9 % NaCl.
Conclusions: The present results are confirmatory of previous studies, in that D-enantiomeric AMPs exhibit more potent antibacterial properties than L-enantiomeric AMPs against *E. faecalis* biofilms within the canal space. Nevertheless, the potency of both AMPs are concentration-dependent. Incorporation of these agents into EDTA, a non-antibacterial calcium-chelating irrigant for removal of the inorganic component of the canal space debris, does not reduce the efficacy of either AMP.
Clinical Significance: The present study provides the proof of concept that incorporation of an antimicrobial peptide into a calcium-chelating root canal irrigant enhances the disinfection of intratubular single-species biofilms during smear layer and smear plug removal.

1. Introduction

Persistent apical periodontitis is a biofilm-induced inflammatory periradicular disease that persists after root canal treatment [1]. Epidemiological studies of root-treated teeth identified a relatively high incidence of post-treatment periradicular lesions, ranging from 16 % to 65 %, depending on the study population and type of teeth included [2]. These infections can be extremely painful and potentially dangerous, leading to localised periradicular lesions, spreading of the dental infection to tissue spaces, or tooth loss [3]. Microbial invasion of the blood circulation during their pathogenesis, treatment or healing phase may cause potentially deadly diseases such as mediastinitis [4], fatal necrotising fasciitis [5] or brain abscess [6].

Biofilms are complex microbial communities that are adherent to

* Corresponding authors at: The Dental College of Georgia, Augusta University, Augusta, GA, USA.
** Corresponding author.
E-mail addresses: niulina831013@126.com (L.-n. Niu), majingzhi2002@163.com (J.-z. Ma), ftay@augusta.edu (F.R. Tay).

https://doi.org/10.1016/j.jdent.2019.103231
Received 15 October 2019; Received in revised form 6 November 2019; Accepted 7 November 2019
0300-5712/ Published by Elsevier Ltd.

each other and/or to surfaces. Bacteria within biofilms are embedded in a self-produced matrix of extracellular polymeric substances, consisting of polysaccharides, proteins, metabolites and extracellular DNA [7]. Biofilm formation is not only the natural mode of survival of many microorganisms, but is also an important clinical pathogenic mechanism, accounting for at least 65 % of all human infections [8]. Biofilms may be up to 1000-fold more resistant to disinfecting agents than their planktonic counterparts; their formation and dispersal are at the root of many persistent and chronic bacterial infections [9].

The goal of root canal treatment is to eliminate microbial biofilms and their by-products from the canal system. However, a large proportion of the canal wall is untouched by contemporary instrumentation techniques [10]. The presence of morphological irregularities, such as isthmuses and cul-de-sacs, makes it challenging to completely disinfect the root canal system, leaving a mass of biofilm-infected dentine surfaces [11]. Apart from biofilms, these hard-to-reach areas may be packed with dentine debris, which are generated and pushed into the dentinal tubules by shaping instruments and may impede the penetration of irrigants and reduce their efficacy [12].

The most commonly used irrigants in endodontics are sodium hypochlorite (NaOCl) and ethylenediammine tetra-acetic acid (EDTA). Sodium hypochlorite is both an oxidizing and hydrolysing agent, displaying potent bactericidal, biofilm-disrupting and tissue-dissolution activities [13]. However, NaOCl demonstrates no effect on the inorganic portion of dentine debris and smear layer, and can cause ecchymosis, paraesthesia or even life-threatening accidents when it is used inadvertently [13]. As a strong chelating agent, EDTA dissolves the inorganic portion of smear layer, but possesses no or only weak antimicrobial activity [14]. To date, none of the currently available irrigating solutions satisfy all the requirements of an ideal irrigant [15]. The clinical dilemma of eliminating persistent endodontic infections highlights the urgent need for the development of novel anti-biofilm compounds.

Antimicrobial peptides (AMPs) are short cationic host-defence molecules that provide the early stage of protection against invading microbes. They also have important inflammatory modulatory roles and act as a bridge between innate and acquired immunity. They are considered potential alternatives to conventional pharmaceuticals against multidrug-resistant pathogens and biofilm-related infections. This is attributed to their broad-spectrum anti-biofilm activities and relatively low bacterial resistance [16]. Antimicrobial peptides can be natural or synthetic; most of them share a cationic amphipathic character, which can be attracted to negative charges on the bacterial surface by electrostatic attraction and destroy the integrity of bacterial membranes [17].

Innate defence regulator peptide-1018 (IDR-1018) is a synthetic 12-amino-acid L-enantiomeric peptide modified from the bovine neutrophil host defence peptide bactenecin [18]. The AMP IDR-1018 modulates the immune system by affecting macrophage polarisation and inhibiting lipopolysaccharide-induced cytokine production. It also disperses biofilms, kills bacteria and inhibits bacterial swarming [19]. Another AMP, DJK-5, is a more recently developed D-enantiomeric protease-resistant peptide. It demonstrates potent anti-biofilm activities against both Gram-positive and Gram-negative bacteria in biofilms [20]. DJK-5 and the mixture of DJK-5 and EDTA have been shown to be effective in killing bacteria in oral multi-species and *E. faecalis* biofilms formed on dentine blocks, hydroxyapatite or titanium disks *in vitro* [20,21]. Both 1018 and DJK-5 are synthetic cationic peptides, and work by binding to and triggering the degradation of the intracellular alarmone nucleotides guanosine tetraphosphate (ppGpp) and pentaphosphate (pppGpp). These molecules, collectively known as (p)ppGpp, are stress-induced second messenger nucleotides and play an important role in the inhibition of biofilm development [22,23].

in vitro anti-biofilm studies on root canal irrigants were mainly implemented in decoronated roots [24], re-approximated root halves [25], dentine blocks and sections [26,27]. To date, no study has investigated the *in-situ* biofilm removal efficacy from 'real' root canal systems using anti-biofilm peptides. Recently, the authors have established a standardised *in-situ* biofilm model of *E. faecalis* in the isthmus, canals and dentinal tubules of single-rooted human maxillary premolars [28]. In the present study, the bactericidal and biofilm-disruption capability of IDR-1018 (10, 20 μg/mL), DJK-5 (10, 20 μg/mL), and a mixture of 17 % EDTA and 1018 (10 μg/mL) or DJK-5 (10 μg/mL) against *in-situ E. faecalis* biofilms grown in the isthmus, canals and dentinal tubules were investigated using the aforementioned biofilm model. The null hypotheses tested were: 1) both AMPs are equally effective in elimination of *E. faecalis* biofilms from different locations of the canal space, and 2) incorporation of either AMP into EDTA as a final irrigant has no adverse effect on the anti-biofilm activity of the corresponding AMP.

2. Materials and methods

2.1. Peptide synthesis

The IDR-1018 (VRLIVAVRIWRR-NH2) and DJK-5 (VQWRAIRVRVIR-NH2) were synthesised by GenScript (Piscataway, NJ, USA), as previously described [22]. Briefly, the peptides were assembled by stepwise solid-phase synthesis using a standard 9-fluorenylmethoxy carbonyl (F-moc) strategy and purified to a purity of > 95 % using reverse-phase high-performance liquid chromatography (RP-HPLC). A peptide stock solution (100 μg/mL) was made by suspending the powder in deionised water.

2.2. Specimen preparation and isthmus identification

Freshly extracted, intact, human single-rooted maxillary premolars were collected based on a protocol approved by the Human Assurance Committee of the corresponding author's university. Ninety-one specimens, each containing two root canals connected by an isthmus, and one shared apical foramen, as determined with a surgical microscope, were included in the present study. The crown of each tooth was resected, leaving a root segment with a standardised length of 18 mm. The root canals were shaped using ProTaper Gold nickel-titanium rotary instruments (Dentsply Sirona Endodontics, Tulsa, OK, USA) to size F3 and irrigated with 2 mL of 6 % NaOCl at each instrument change. Each canal was rinsed with 3 mL of 5 % sodium thiosulfate to neutralise the residual NaOCl [29], and subsequently irrigated with 5 mL of QMix 2 in. (Dentsply Sirona Endodontics) for the removal of smear layer and smear plugs. This was followed irrigation with a copious amount of 0.9 % NaCl. All these procedures were performed by a single trained operator.

Two longitudinal grooves were created along the buccal and palatal ridges of each specimen, without exposing the canal system, for tooth-splitting purpose. Each isthmus was labelled by preparing three transverse grooves on the palatal ridge, one at the cementoenamel junction and the other two on the root surface, dividing the root into three parts of equal length (Fig. 1A). The root segment of each specimen was embedded in polyvinylsiloxane impression material (Dentsply Sirona, York, PA, USA) in a 5-mL microcentrifuge tube to simulate a closed canal system (Fig. 1B) [30]. Each tube was subsequently filled with 1.5 mL of brain heart infusion broth (BHI; MilliporeSigma, St. Louis, MO, USA) and autoclaved for sterilisation.

2.3. In-situ biofilm formation in the root canal system

A single colony of *E. faecalis* (ATCC 29212, American Type Culture Collection, Manassas, YA, USA) was propagated in 10 mL sterile BHI broth at 37 °C for 5 h to obtain a mid-exponential suspension. The optical density (OD) at 600 nm was spectrophotometrically adjusted to 0.5, equivalent to 1×10^8 cells/mL [31], to generate an inoculum suspension. Each sterilised root segment was inoculated with *E. faecalis*

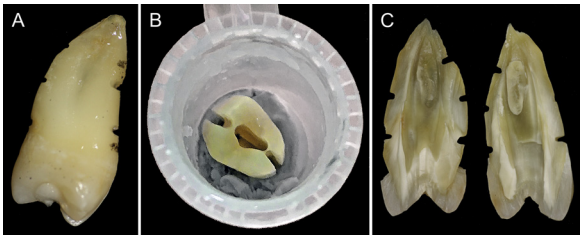

Fig. 1. Specimen preparation, marking and splitting. **A**. A specimen with bur notches trisecting the roots and locating the isthmus area. **B**. Embedding of the specimen in polyvinylsiloxane impression material in a 5 mL micro-centrifuge tube for bacteria inoculation and culture of biofilm. **C**. Split infected tooth-halves for CLSM in the isthmus and canal regions.

suspension by using a sterile 200-μL pipette tip. The root segment was immersed in inoculum by placing two additional mL of bacterial suspension into each tube. All specimens were subsequently incubated aerobically at 37 °C for 4 weeks to allow biofilm development in the closed canal system, with the broth replaced every 48 h.

2.4. Taylor-modified Brown and Brenn staining for light microscopy

A cylindrical dentine block containing a narrow isthmus was obtained by resecting the crown and the apex of one randomly-selected infected specimen. The dentine block was fixed with 4 % paraformaldehyde, demineralised completely in 10 % formic acid/sodium formate, embedded in paraffin and sectioned transversely. The dentine sections were stained for bacteria using the Taylor-modified Brown and Brenn technique [32]. Examination was performed with light microscopy (20x magnification; Axioplan 2 Fluorescence Imaging; Zeiss, Germany) for qualitative evaluation of biofilm bacteria within the dentinal tubules (note: canal wall biofilms were dislodged during specimen processing).

2.5. Anti-biofilm treatments

The remaining 90 infected specimens were randomly divided into the 9 groups (N = 10): (1) 0.9 % NaCl (negative control); (2) 17 % EDTA (test control); (3) 10 μg/mL 1018; (4) 10 μg/mL 1018 + 17 % EDTA; (5) 20 μg/mL 1018; (6) 10 μg/mL DJK-5; (7) 10 μg/mL DJK-5 + 17 % EDTA; (8) 20 μg/mL DJK-5; (9) 6 % NaOCl (positive control). For all groups, each canal of the specimen was irrigated with 6 mL of the aforementioned solution for 60 s, in an up-and-down motion with the needle stopping 1 mm short of binding. For the positive control, each specimen was further irrigated with 4 mL 5 % sodium thiosulfate to neutralise the NaOCl. A final rinse with sterile saline was performed and the total volume of irrigating solution for each specimen was standardised to 20 mL. All irrigating procedures were performed with a 30-gauge side-vented needle (ProRinse®, Dentsply Sirona Endodontics).

2.6. Bacterial sampling and colony-forming unit counting

Bacterial samples were taken before (S1) and immediately after (S2) anti-biofilm treatments, from a randomly chosen canal of each specimen, as previously described [33]. Briefly, the canal wall was vigorously disrupted using a size 35 K-file for 30 s and rinsed with 500 μL of phosphate buffered saline (PBS). The canal contents were aspirated with a 1 mL syringe and transferred to a tube containing 2 mL of PBS, which was subsequently sonicated for 60 s and serially-diluted.

Fifty-microlitre aliquots were inoculated onto BHI agar and incubated aerobically for 48 h. The colony-forming units (CFUs) cultivated were determined and transformed into actual counts based on the dilution factor. Reductions of intracanal bacteria load (in CFU/mL) was expressed as percentage reductions and log-reductions after $\log_{10}$-transformation of the CFU counts.

2.7. Confocal laser scanning microscopy

After post-treatment bacterial sampling (S2), each specimen was split longitudinally into two halves (mesial and distal halves) using a hammer and a razor blade (Fig. 1C). One split half from each group were further transversely sectioned across the isthmus region to expose the dentinal tubules. For each of the 9 groups, the freshly exposed dentine section and five randomly chosen half of a split specimen were stained with LIVE/DEAD BacLight Bacterial Viability Kit (L-7012, Molecular Probes, Eugene, OR, USA) for 15 min and then rinsed gently with PBS. Three randomly-selected areas (212.34 μm x 212.34 μm each) of the fluorophore-stained biofilms on the dentine surface of the isthmus, the canal and the dentinal tubules were examined by confocal laser scanning microscopic imaging (CLSM; LSM 780 multiphoton, Carl Zeiss, Germany), as previously described (N = 15 for canal surface biofilms; N = 3 for dentinal tubules) [28]. Three-dimensional volume stacks were acquired for each scanned area with a 0.5-μm step size using the Zen Black software (Carl Zeiss). The percentage of dead bacteria was calculated by using the BioImage L software (Department of Oral Biology, Malmo University, Sweden) and the thickness of treated biofilms was determined with Image Pro Plus (Media Cybernetics, Rockville, MD, USA).

2.8. Quantitation of dehydrogenase activity of treated E. faecalis

The effect of antimicrobial peptides on dehydrogenase activity of *E. faecalis* was evaluated using the XTT Cell Proliferation Kit II (Roche Diagnostics, Mannheim, Germany). This assay utilises the reduction of the yellow tetrazolium salt 2,3-bis(2-methoxy-4-nitro-5-sulphophenyl)-2H-tetrazolium-5-carboxanilide (XTT) by dehydrogenases in metabolically-active cells to a water-soluble orange formazan dye, the density of which is directly proportional to the overall dehydrogenase activity of live cells [34]. Briefly, 100 μL of *E. faecalis* suspension from tube S2 was added to a 24-well plate and exposed to XTT labelling mixture (final concentration 0.3 mg/mL) in the dark at 37 °C for 4 h. Formazan was spectrophotometrically determined using a microplate reader (Bio-Rad, Model 2550, Richmond, CA, USA) at 492 nm with a reference wavelength at 690 nm. The OD values for the wells without biofilms served as blank control.

2.9. Lactic acid production

Lactic acid levels of *E. faecalis* treated by the experimental and control root canal irrigants were evaluated using an enzymatic method (lactate dehydrogenase). Two hundred microlitres of *E. faecalis* suspension from tube S2 was incubated in a 24-well plate for 48 h to produce biofilms, followed by addition of 1 mL of buffered peptone water (BPW) supplemented with 0.2 % sucrose, which was subsequently incubated at 37 °C for 3 h to produce lactic acid. The lactate concentrations in the BPW solutions were evaluated using the L-Lactic Acid Assay Kit (Megazyme, Wicklow, Ireland). The OD values at 340 nm (OD_{340}) was measured as previously described [35]. A single-point standard (lactic acid, 0.15 g/L) was performed concurrently with each batch of samples.

2.10. Determination of biofilm polysaccharide levels

A phenol-sulphuric acid method was used to detect the water-insoluble polysaccharides produced by *E. faecalis* biofilms [36]. Two hundred microlitres of *E. faecalis* suspension from sample S2 was incubated in a 1.5 mL tube for 48 h to develop biofilms, which was subsequently centrifuged at 12,000 *g* for 2 min. After removal of the supernatant solution, the precipitate was re-suspended in 200 μL of deionised water, supplemented with 200 μL of 5 % phenol and 1 mL of 97 % sulphuric acid, and then incubated for 30 min. Subsequently, 100 μL aliquots of the incubated mixture were added to a 96-well plate

for measuring the OD values at 490 nm ($OD_{490\ nm}$). Six glucose concentrations (0, 5, 10, 20, 50 and 100 mg/L; MilliporeSigma, St. Louis, MN, USA) were used as standard values in the conversion of $OD_{490\ nm}$ to polysaccharide concentrations.

2.11. Statistical analyses

Biofilm evaluation (CFU, XTT, CLSM) and the corresponding statistical analysis were performed by other researchers who were blinded with respect to the group designations. For each parameter, data sets were tested for their normality and homoscedasticity assumptions prior to the use of parametric statistical methods. If those assumptions appeared to be violated, the corresponding data sets were nonlinearly-transformed to satisfy those assumptions prior to the use of one-factor or two-factor analysis of variance (ANOVA) and Holm-Šidák pairwise comparison procedure. If those assumptions remained violated after multiple nonlinear assumptions, Kruskal-Wallis ANOVA and Dunn's pairwise comparison procedure was employed for analyses. For all tests, statistical significance was set at $\alpha = 0.05$. The IBM® SPSS 25.0 software package (IBM, Armonk, NY, USA) was used for statistical analysis.

3. Results

A dense, multi-layered, mature biofilm with a predominant proportion of live (green) bacteria and miniscule dead (red) bacteria on dentine surfaces of the isthmus and the corresponding canals were confirmed by CLSM (Fig. 3A – 0.9 % NaCl panel) after 4 weeks of incubation. Penetration of *E. faecalis* biofilms into the dentinal tubules was demonstrated by both light microscopy (Fig. 2) and CLSM (Fig. 4A – 0.9 % NaCl panel), with most of the tubule openings blocked with bacteria and a maximum penetration depth of 782 µm.

Compared to 0.9 % NaCl (negative control), 17 % EDTA (test control) demonstrated almost no effect on the biofilm structures in the root canal system (Fig. 3A – 17 % EDTA panel). Compared with the negative and test controls, the AMPs 1018, DJK-5, or mixtures of 17 % EDTA with either AMP disrupted canal wall surface biofilms in the isthmuses and canals to varying degrees, while 6 % NaOCl (positive control) extensively disrupted and almost completely eliminated the biofilms (Fig. 3A). Consequently, biofilm thickness in the positive control group could not be measured and was excluded from the statistical analysis. Biofilm thickness of the other 8 groups was between 11 − 12 µm in both regions, and were not significantly affected by the factor "irrigant" ($p = 0.568$) or "location" ($p = 0.558$; two-factor ANOVA) (Fig. 3B). The interaction of these two factors was not significant ($p = 0.978$).

The percentages of dead bacteria in the biofilms present in the isthmuses and canals were significantly affected by the factor "irrigant ($p < 0.001$), but not by the factor "location" ($p = 0.157$). No significant interaction between the two factors was identified ($p = 0.707$). On the average, 7.89 % and 6.42 % of the bacteria in the artificially-developed biofilms in the isthmus and corresponding canal were dead

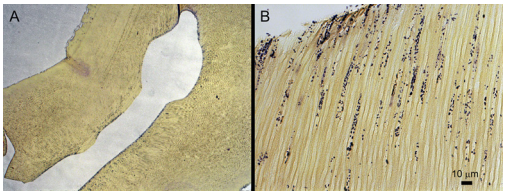

Fig. 2. Representative Taylor-modified Brown and Brenn-stained light microscopy images of *E. faecalis* within the dentinal tubules of an instrumented premolar tooth with artificially-infected root canals. Biofilms on dentine surfaces of the isthmus and canals were disrupted during processing prior to staining and can be better appreciated with CLSM imaging (Fig. 3). **A**. Buccal canal and isthmus (2.5x magnification). **B**. High magnification of intratubular bacteria (40x magnification).

in the NaCl negative control group (Fig. 3A and 3C). The AMPs 1018, DJK-5 or mixtures of EDTA with either AMP killed biofilm bacteria in the isthmuses and corresponding canals (Fig. 3A), with a percentage kill ranging from 16.75 to 57.31 %, depending on the peptide type and concentration (Fig. 3C). At any concentration, DJK-5 was significantly more effective in bacteria killing than 1018 ($p < 0.001$). For each peptide, a higher concentration resulted in significantly more effective killing ($p < 0.001$). For any irrigating solution used in the present study, no significant difference in bacteria killing was found between the two locations (isthmus or canal) ($p > 0.05$).

Both 1018 and DJK-5 demonstrated strong biofilm bacteria killing in the dentinal tubules (Fig. 4A). The percentage of biofilm bacteria killed was in the ascending order: 0.9 % NaCl (6.3 ± 0.8 %) = 17 % EDTA (6.5 ± 0.5 %) < 10 µg/mL 1018 (19.2 ± 3.1 %) = 10 µg/mL 1018 in EDTA (21.2 ± 1.0 %) < 20 µg/mL 1018 (27.5 ± 1.6 %) < 10 µg/mL DJK-5 (35.0 ± 2.6 %) = 10 µg/mL DJK-5 in EDTA (36.0 ± 4.2 %) > 20 µg/mL DJK-5 (55.8 ± 2.8 %) < 6 % NaOCl (91.0 ± 4.3 %) ($p < 0.01$) (Fig. 4B).

The overall mean CFU counts obtained by K-file before anti-biofilm treatment was 1.66×10^{10} CFU/mL and no significant difference was found among the nine groups ($p > 0.05$; data not shown). After irrigation, the percentage reduction of CFUs in the negative control (0.9 % NaCl, 75.71 ± 6.18 %) and test control (17 % EDTA, 76.08 % ± 5.98 %) was not significantly different ($p > 0.05$). Both groups had considerably lower CFU reduction than the other 7 groups (99–100% reduction) ($p > 0.05$; data not shown). Log-reduction of the CFU counts are shown in Fig. 5A. One-factor ANOVA analysis of log reduction of CFUs counts indicated a significant difference ($p < 0.001$), in the descending order (folds): 6 % NaOCl (5.69 ± 0.14) > 20 µg/mL DJK-5 (3.70 ± 0.15) > 10 µg/mL DJK-5 (2.84 ± 0.16) = 10 µg/mL DJK-5 in 17 % EDTA (2.81 ± 0.13) > 20 µg/mL1018 (2.49 ± 0.14) > 10 µg/mL 1018 (1.92 ± 0.13) = 10 µg/mL 1018 in 17 % EDTA (1.93 ± 0.14) > 17 % EDTA (0.63 ± 0.11) = 0.9 % NaCl (0.63 ± 0.11) ($p < 0.001$).

The OD values of the XTT assays are summarised in the box-and-whisker plot in Fig. 5B. These values were normalised against the negative control for statistical analysis. Compared with the negative and test controls, 1018, DJK-5 and 6 % NaOCl greatly reduced the dehydrogenase activities of *E. faecalis* biofilms ($p < 0.001$). Lactic acid and polysaccharide production by *E. faecalis* biofilms are shown in Fig. 5C and D, respectively. For both metabolic products, significant differences were observed among different groups ($p < 0.001$; Kruskal Wallis ANOVA). Both lactic acid and polysaccharide production were in the order: 0.9 % NaCl = 17 % EDTA > 10 µg/mL 1018 = 10 µg/mL 1018 in EDTA ≥ 20 µg/mL 1018 = 10 µg/mL DJK-5 = 10 µg/mL DJK-5 in EDTA ≥ 20 µg/mL DJK-5 > 6 % NaOCl ($p < 0.05$). No significant difference was found between 10 µg/ml DJK-5 and 20 µg/ml 1018 ($p > 0.05$).

Although 17 % EDTA possessed negligible bacterial killing activity, it did not alter the anti-biofilm efficacy of either AMP, or adversely affect the suppression of *E. faecalis* metabolic activity by the AMPs after their incorporation into the irrigant.

4. Discussion

Persistent endodontic infection is a microbe-induced inflammatory disorder, predominantly caused by microbial biofilms that remain deep-seated in the previously-treated root canal system or on the extra-radicular surface [37]. Bacterial biofilms causing persistent intraradicular inflammation are usually located in areas that are difficult to be accessed by instruments and irrigants, such as the root canal isthmus. An isthmus is a narrow, ribbon-shaped communication connecting two root canals that may hide necrotic pulp tissues, biofilms or residual filling material [38]. Any root that contains two canals or C-shaped canal has the potential to contain an isthmus. The recognition and treatment of isthmuses may be one factor that reduces the failure

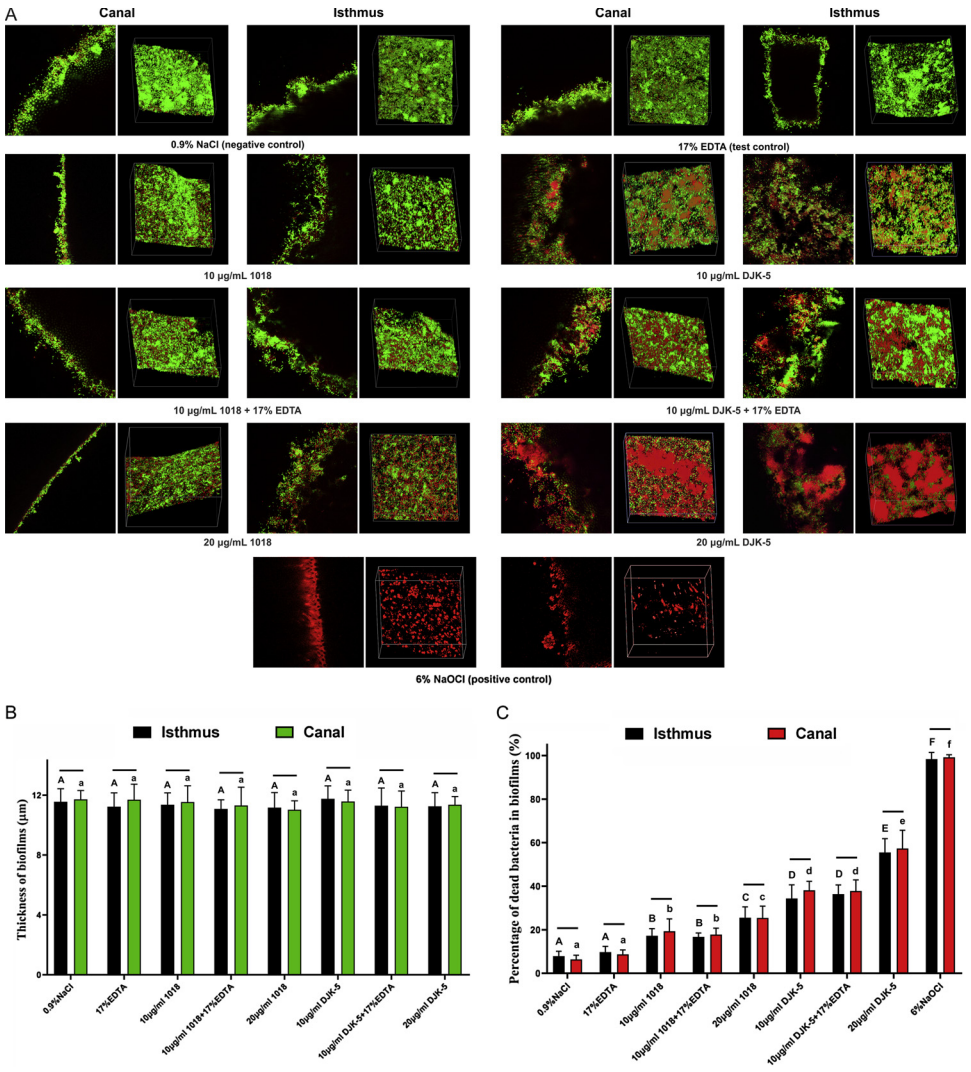

Fig. 3. A. Representative CLSM images of live/dead-stained *E. faecalis* biofilms on isthmus and canal walls after irrigation with one of the nine irrigating solutions. For each set of images, the left and right images represent 2D structures and 3D volume stacks, respectively. **B.** Bar chart summarising the biofilm thickness in the different groups. Values are means and standard deviations (N = 15). Isthmus columns (in black) labelled with the same upper case letters are not significantly different ($p > 0.05$). Canal columns (in red) labelled with the same lower case letters are not significantly different ($p > 0.05$). For each irrigant, isthmus and canal columns labelled with a horizontal bar are not significantly different ($p > 0.05$). **C.** Bar chart depicting the percentages of dead bacteria in *E. faecalis* biofilms treated with different irrigants. Values are means and standard deviations (N = 15). Isthmus columns (in black) labeled with different upper case letters are significantly different ($p < 0.05$). Canal columns (in red) labelled with different lower case letters are significantly different ($p < 0.05$). For each irrigant, isthmus and canal columns labeled with a horizontal bar are not significantly different ($p > 0.05$) (For interpretation of the references to colour in this figure legend, the reader is referred to the web version of this article.).

rate of root canal treatment [39]. In the present study, a standardised single-species biofilm model was established in the isthmus and the corresponding canals of single-rooted maxillary premolars after 4-week of incubation, prior to evaluating the anti-biofilm efficacy of AMPs.

Biofilm 'life cycle' consists of bacterial attachment to a surface, development of micro-colonies that are connected by a network of water channels [40], maturation, and finally detachment and dispersal from a mature biofilm as free planktonic bacteria [8,41]. In the present study, approximately 7 % of the bacteria in artificially-established biofilms in the root canal system (negative control) were dead, implying that cell death occurs during biofilm development. Cell death plays an important role in subsequent differentiation within biofilms, creating voids inside the micro-colonies and dispersal of cells from within these voids [40]. Dispersal events are generally thought to benefit the biofilm by releasing phenotypically-diverse cells for the colonisation of new surfaces, limiting overcrowding in a densely-populated and genetically-diversified mature biofilm, and reinitiating the biofilm life cycle [42]. Biofilm dispersal from the root canal system or the extraradicular surfaces may worsen the infection and provide a persistent source of root canal infection [9,43].

Biofilm dispersal mechanisms mainly include enzymatic-induced matrix-degrading mechanisms and broad-spectrum dispersal mechanisms. The former consists of protease-mediated degradation of the proteinaceous matrix component [44], nuclease-mediated degradation of eDNA [45] and dispersin B-mediated degradation of the polysaccharide matrix component [46]. The latter consists of inhibition of D-amino-acid-mediated protein synthesis [47], stringent response inhibition [22] and surfactant-mediated dispersal [48].

Results of the present work are confirmatory of previous studies by Dr. Haapasalo's group [21,49], in that the D-enantiomeric AMP exhibits potent antibacterial properties against canal space *E. faecalis* biofilms. The difference between the present work and previous studies is that both D-enantiomeric and L-enantiomeric AMPs were tested in the same study under the same experimental conditions, and that the biofilms were cultured inside irregular root canals and isthmuses of human teeth in a closed canal system, instead of flat, bovine collagen-coated hydroxyapatite disks [21] or sectioned root canal dentin blocks [49] in which the biofilms are readily exposed to the AMP-containing irrigants. While the present results are confirmatory in nature, performing irrigation within a root canal system with a communicating isthmus is more clinically relevant that using hydroxyapatite discs or sectioned dentine blocks. In addition, some parts of the canal space may not be reached by a root canal irrigant in a closed canal model [50,51]. Thus, CLSM evaluation of biofilms within the canal space alone may yield results that are different from those derived from explicitly-exposed dentin blocks. To address such an issue, other biofilm evaluation methods, including quantification of CFUs, XTT assay, lactate dehydrogenase assay and phenol-sulphuric acid evaluation of biofilm polysaccharide levels were used in the present work to supplement the CLSM results.

Compared with 6 % NaOCl (positive control), both the L-enantiomeric AMP 1018 and the L-enantiomeric AMP DJK-5 could not

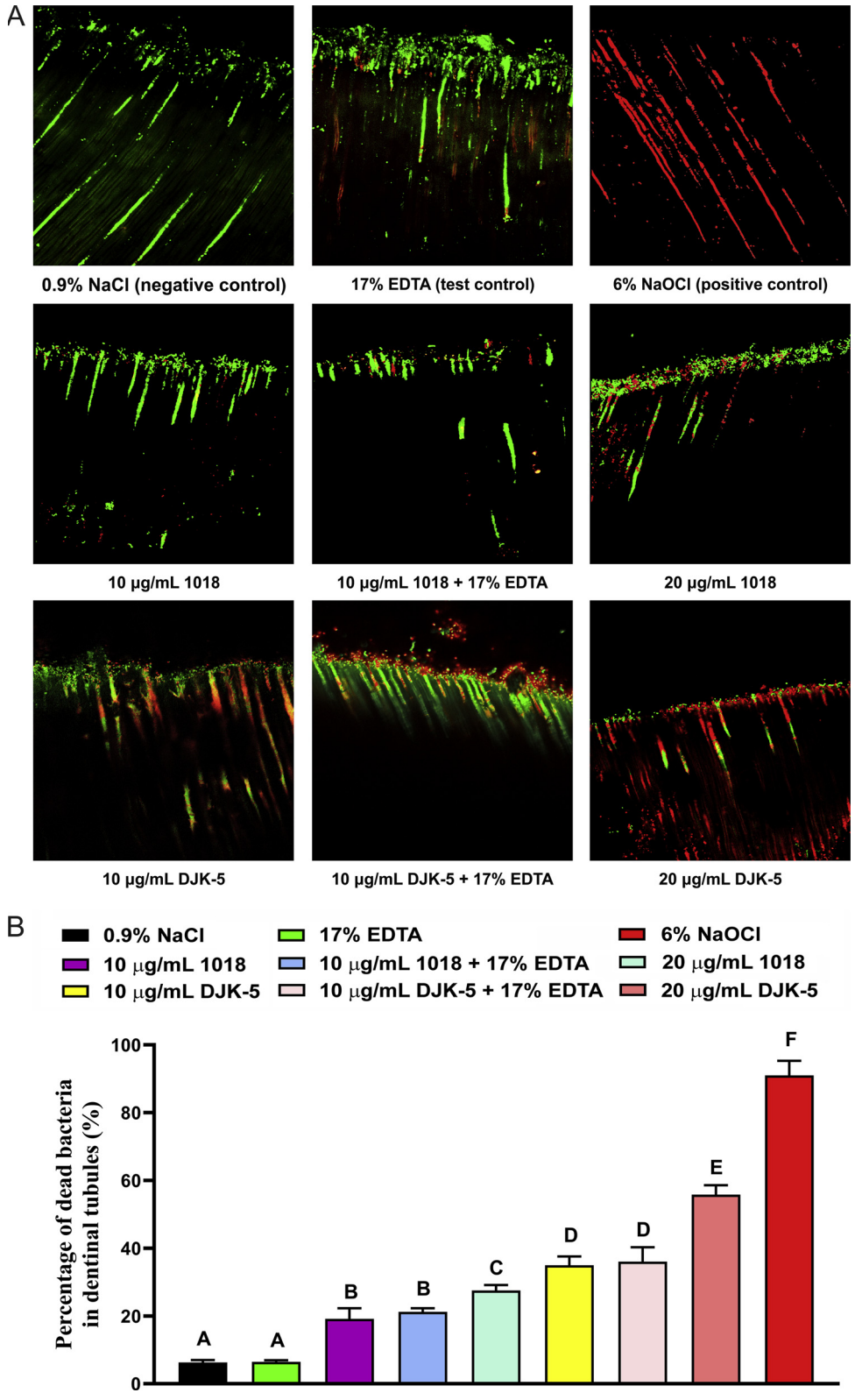

Fig. 4. A. Representative 3D merged CLSM images of live/dead-stained *E. faecalis* within the dentinal tubules of artificially-infected root canals treated with different irrigating solutions. **B**. Bar chart depicting the percentages of dead bacteria within the dentinal tubules. Values are means and standard deviations (N = 15). Columns labelled with different upper case letters are significantly different ($p < 0.05$).

eradicate the 4-week old *E. faecalis* biofilms in root canal system, irrespective of whether they are incorporated in 17 % EDTA. Although the biofilm thickness was not significantly altered by AMPs or mixtures of EDTA and either peptide, the biofilm structures were partially-disrupted and biofilm bacteria were potently killed within the root canals, isthmuses and dentinal tubules after 1-min irrigation of each canal. These observations are similar to the findings from previous studies in which biofilms were performed on hydroxyapatite disks, and

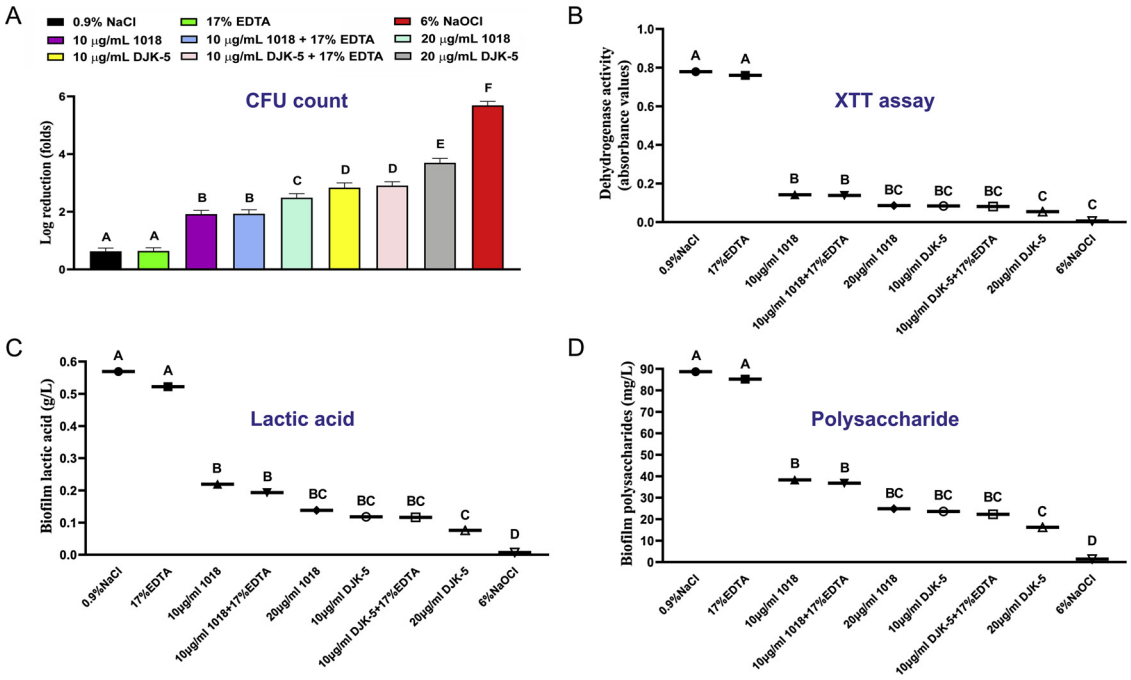

Fig. 5. Effects of irrigating solutions on CFUs reduction, dehydrogenase activity, lactic acid and polysaccharide production of post-treatment sample (S2). **A**. Bar chart showing the $\log_{10}$ reduction of CFUs counts. Values are means and standard deviations (N = 10). **B**. Box-and-whisker plot depicting mitochondrial dehydrogenase activity derived from XTT assays. Values are medians and percentiles (N = 10). **C**. Box-and-whisker plot quantifying lactic acid production of *E. faecalis* biofilms (in g/L). Values are medians and percentiles (N = 10). **D**. Box-and-whisker plot depicting polysaccharide synthesis of *E. faecalis* biofilms (in mg/L). Values are medians and percentiles (N = 10). For each chart, columns identified with different upper letters are significantly different ($p < 0.05$).

the anti-biofilm activity of peptides were concentration-dependent [20,52]. The residual live bacteria and extracellular polymeric substances in biofilms partially-disrupted by AMPs could be a good source and support for new biofilm formation.

The immunomodulatory activities of synthetic immunomodulatory innate defence regulators (IDRs) are reflected in part by their ability to induce chemokines in peripheral blood mononuclear cells (PBMCs) [53]; this activity is related to their ability to protect against infections [54]. Peptide 1018 showed more than 10-fold enhanced chemokine induction capability compared with the synthetic peptide IDR-1 [55,56] and much greater activities than the sequence scrambled parent Bac2A which caused only a 3-fold increase in MCP-1 concentration at 100 ug/mL [57].

The potential cytotoxicity of the AMPs at relative high concentrations should not be overlooked. IDR-1018 was reported to be non-toxic at concentrations higher than the ones used in the present study [57,58]. At 375 μg/mL of 1018, only a slight toxic effect was observed with lysis of 14.4 % of the red blood cells after a 24-h exposure period [57]. At concentrations of 20 μg/mL and 100 μg/mL, no lytic effect of red blood cells was observed. At concentrations of up to 200 μg/mL, no release of lactate dehydrogenase was detected from human PBMCs. Both of these results are indicative of the relative absence of cytotoxicity [57,58]. DJK-5 has been shown to cause tissue damage *in vivo* at concentrations above 1500 μg/mL; however, no obvious signs of inflammation or tissue necrosis were observed for formulated nanogels containing 3000, 4500 or 6000 μg/mL of DJK-5 [59]. Inflammation was only evident after the incorporation of 7500 μg/mL of DJK-5 in the nanogels [59]. The low cytotoxicity of cationic AMPs has been attributed to the inherent structural and functional differences in the membranes of mammalian cells and bacterial pathogens. Compared to mammalian cells, bacterial cytoplasmic membranes contain much more anionic components, such as phosphatidylserine and cardiolipin [60].

To-date, three major mechanisms have been suggested for the mode of action of cationic AMPs: electrostatic attraction, transmembrane pore formation and intracellular killing [16,61,62]. The cationic charge of AMPs must first be attracted to negatively-charged surfaces of Gram-negative (outer membrane) or Gram-positive (cell wall) bacteria, which present very different outer surfaces to attacking AMPs [62]. Once cationic AMPs cross the outer barriers of bacteria pathogens, they permeate the phospholipid bilayers of bacterial cell membrane to produce pores via 'toroidal pore', 'carpet' or 'barrel-stave' mechanisms [16,61,62]. In addition, translocated peptides engage in intracellular killing by altering cytoplasmic membrane septum formation, inhibiting cell-wall synthesis, binding nucleic acids, inhibiting nucleic acid synthesis, inhibiting protein synthesis or inhibiting enzymatic activity [16,61,62]. Different from peptides that exert activity by transmembrane pore formation, IDR-1018 and DJK-5 can penetrate into cells, bind to and trigger the degradation of intracellular (p)ppGpp, which are key physiological regulators of the stringent response and play an important role in biofilm formation and maintenance [63]. These intracellular (p)ppGpp are particularly susceptible to intracellular or membrane-bound proteases [64].

All the aforementioned antimicrobial models of AMPs are based on interactions between antimicrobial molecules and the bacterial membrane lipids, without considering the self-assembly or oligomerisation of AMPs. Recent studies demonstrated that cationic amphiphilic peptides possess the ability to self-assemble into supramolecular nanostructures; this property has been exploited to create structures for tissue engineering and drug delivery [65]. Links between the process of AMP self-assembly and antimicrobial activity have recently been suggested [66–68]. Schnaider et al. reported the significance of self-assembled nanostructures of diphenylalanine on bacterial membrane permeation and depolarisation, upregulation of stress response regulons and damage to bacterial morphology [67]. Self-assembly of AMPs on the bacterial membrane cannot be disregarded as a potential mechanism for the antimicrobial activity of these peptides.

The best-studied bacterial resistance strategies against AMPs involve electrostatic repulsion of AMPs by alteration of net surface charge, external sequestration by production of AMP-trapping proteins, active extrusion of AMPs by energy-dependent efflux pumps,

destruction of L-enantiomeric AMPs by proteolytic degradation, as well as the inhibition of host pathways for the production of AMPs [61]. Increases in bactericidal potency of D-amino acid versions of AMPs, compared with their L-amino acid counterparts, are often attributed to their increased stability against enzymatic degradation [23]. This is because bacteria secrete proteases that are composed of L-amino acids. Natural AMPs are often susceptible to proteolytic degradation by host proteases [23]. Incorporation of retro-inverso peptides and D-enantiomer amino acids into AMPs produce D-enantiomeric peptides. These peptides have been shown to be a potent strategy for overcoming the limitations of L-enantiomeric peptides [23,69]. Because D-amino acids are not naturally present in human peptides, this renders the D-enantiomeric peptides less easily recognised by bacterial or host proteases, which are present in large amounts during infection and can degrade AMPs composed entirely of L-amino acids [69,70]. In the present study, DJK-5 displayed considerably more potent anti-biofilm efficacy than 1018 in root canal systems. Accordingly, the first null hypothesis that "both AMPs are equally effective in elimination of *E. faecalis* biofilms from different locations of the canal space" has to be rejected. This difference is probably attributed to the relative ability of D-enantiomeric peptides to penetrate bacterial cells. The resistance of D-enantiomeric peptides to bacterial proteases enhances their capacity to stimulate degradation or prevent accumulation of (p)ppGpp.

The higher antimicrobial potency of D-enantiomers compared to L-enantiomers of AMPs cannot always be attributed to their different resistance to protease degradation [66]. Recently, it has been demonstrated that D-GL13 K is significantly more active than L-GL13 K against Gram-positive bacteria such as *E. faecalis* and *Streptococcus gordonii* [69]. Even with the protease-negative strain *E. faecalis* TX5128, the results showed that the activity of L-GL13 K was also lower than that of D-GL13 K in the absence of bacterial proteases. The result suggests that protease resistance is not the only difference in killing effectiveness of *E. faecalis* between L- and D-enantiomers of AMPs [68]. Additional resistance mechanisms may be present in the Gram-positive bacteria.

The L- and D-amino acid versions of GL13 K, an AMP derived from a human protein, had been investigated for the structural links between AMP secondary structure, supramolecular self-assembly dynamics and antimicrobial activity [66]. The results indicate that pH dependence and the evolution of secondary structures are related to self-assembly, with differences among these AMPs [66]. Both GL13 K enantiomers form analogous self-assembled twisted nanoribbon structures. However, D-GL13 K initiates self-assembly faster and has notably higher antimicrobial potency than L-GL13 K. A non-antimicrobial scrambled amino acid version of L-GL13 K assembled at a much higher pH to form distinctively different self-assembled structures than L-GL13 K. These results suggest a potential functional relationship between self-assembly of AMPs and their antimicrobial activities [66]. Such a relationship may partially account for the difference in antibacterial effects between the D-enantiomer AMP and the L-enantiomer AMP investigated in the present study.

An ideal irrigant should demonstrate not only biofilm disruption, bacterial killing and tissue-dissolution activity, but also other properties such as lubrication, demineralisation and removal of dentinal debris and smear layer [15]. No commercially available irrigant is capable of dissolving organic tissue and demineralising the smear layer simultaneously [71]. Chelating agents such as EDTA is required for the removal of smear layer during root canal preparation [72]. Antagonistic interactions between EDTA and NaOCl results in the reduction of free available chlorine derived from NaOCl, thereby reduces tissue dissolution and to a lesser extent, antimicrobial activity [73]. QMix 2 in. (Dentsply Tulsa Dental Specialities), a mixture consisting of EDTA, chlorhexidine and cetrimide, is effective in smear layer removal and bacteria killing, but is comparatively less effective than NaOCl in biofilm disruption [74]. In the present study, mixtures of EDTA and 1018 or DJK-5 demonstrated the same anti-biofilm effect as either peptide alone. Accordingly, the second null hypothesis that "incorporation of either AMP into EDTA as a final irrigant has no adverse effect on the anti-biofilm activity of the corresponding AMP" cannot be rejected. Because incorporation of the AMPs investigated with EDTA did not adversely affect the effectiveness of 1018 or DJK-5, mixtures of EDTA and AMPs appear to be promising root canal irrigants for further testing. Compared with single-species biofilms, mixed-species biofilms are considerably more virulent because of the synergistic interaction between different bacterial species within a single biofilm structure [75]. These polybacterial biofilms may have different susceptibility to antimicrobial agents [76]. Because biofilms that are involved in root canal infections are polybacterial in nature [77], further evaluations should be contemplated using mixed-species bacterial biofilm models. In addition, the cytotoxicity of AMP-incorporated EDTA solution should be investigated using human cell lines or large animal histological models.

5. Conclusion

With the limits of the present study, it may be concluded that the D-enantiomeric AMP DJK-5 demonstrates significantly more potent anti-biofilm capacity in the canals, isthmuses and dentinal tubules of single-rooted maxillary premolars, compared with the L-enantiomeric AMP 1018. The anti-biofilm activity of both AMPs is concentration dependent. Biofilm killing by DJK-5 is more effective than 1018, but is inferior to 6 % NaOCl. Incorporation of the AMPs in EDTA does not replace the use of NaOCl as the primary irrigant for disinfection and tissue dissolution. Rather, such an endeavour imparts anti-biofilm capability to EDTA when it is used for dissolution of the smear layer and smear plugs after the application of NaOCl. This is important for eliminating intratubular bacteria that are not readily accessible by NaOCl prior to the removal of the inorganic component of the smear layer.

Declaration of Competing Interest

The authors deny any conflict of interest.

Acknowledgements

The authors declare no conflict of interest associated with the present study. The study was supported by grant 81873714 (PI: Jingzhi Ma), grant 81720108011 (PI: Franklin Tay), grants 81722015 and 81870805 (PI: Li-na Niu) from the National Natural Science Foundation of China.

References

[1] M. Haapasalo, Y. Shen, D. Ricucci, Reasons for persistent and emerging post-treatment endodontic disease, Endod. Topics 18 (2011) 31–50.
[2] I.F. Persoon, A.R. Özok, Definitions and epidemiology of endodontic infections, Curr. Oral Health Rep. 4 (2017) 278–285.
[3] W.W. Hsiao, K.L. Li, Z. Liu, C. Jones, C.M. Fraser-Liggett, A.F. Fouad, Microbial transformation from normal oral microbiota to acute endodontic infections, BMC Genomics 13 (2012) 345.
[4] H. Pappa, D.C. Jones, Mediastinitis from odontogenic infection. A case report, Br. Dent. J. 198 (2005) 547–548.
[5] M. Umeda, T. Minamikawa, H. Komatsubara, Y. Shibuya, S. Yokoo, T. Komori, Necrotizing fasciitis caused by dental infection: a retrospective analysis of 9 cases and a review of the literature, Oral Surg. Oral Med. Oral Pathol. Oral Radiol. Endod. 95 (2003) 283–290.
[6] M.A. Corson, K.P. Postlethwaite, R.A. Seymour, Are dental infections a cause of brain abscess? Case report and review of the literature, Oral Dis. 7 (2001) 61–65.
[7] P. Stoodley, K. Sauer, D.G. Davies, J.W. Costerton, Biofilms as complex differentiated communities, Annu. Rev. Microbiol. 56 (2002) 187–209.
[8] L. Hall-Stoodley, J.W. Costerton, P. Stoodley, Bacterial biofilms: from the natural environment to infectious diseases, Nat. Rev. Microbiol. 2 (2004) 95–108.
[9] J.W. Costerton, P.S. Stewart, E.P. Greenberg, Bacterial biofilms: a common cause of persistent infections, Science 284 (1999) 1318–1322.
[10] Z. Metzger, R. Zary, R. Cohen, E. Teperovich, F. Paqué, The quality of root canal preparation and root canal obturation in canals treated with rotary versus self-adjusting files: a three-dimensional micro-computed tomographic study, J. Endod. 36 (2010) 1569–1573.

[11] L. Susin, Y. Liu, J.C. Yoon, J.M. Parente, R.J. Loushine, D. Ricucci, T. Bryan, R.N. Weller, D.H. Pashley, F.R. Tay, Canal and isthmus debridement efficacies of two irrigant agitation techniques in a closed system, Int. Endod. J. 43 (2010) 1077–1090.

[12] J.F. Sequeira Jr., F.R. Alves, M.A. Versiani, I.N. Rôças, B.M. Almeida, M.A. Neves, M.D. Sousa-Neto, Correlative bacteriologic and micro-computed tomographic analysis of mandibular molar mesial canals prepared by self-adjusting file, reciproc, and twisted file systems, J. Endod. 26 (2013) 1044–1050.

[13] W.C. Zhu, J. Gyamfi, L.N. Niu, G.J. Schoeffel, S.Y. Liu, F. Santarcangelo, S. Khan, K.C. Tay, D.H. Pashley, F.R. Tay, Anatomy of sodium hypochlorite accidents involving facial ecchymosis - a review, J. Dent. 41 (2013) 935–948.

[14] D.R. Drake, A.H. Wiemann, E.M. Rivera, R.E. Walton, Bacterial retention in canal walls in vitro: effect of smear layer, J. Endod. 20 (1994) 78–82.

[15] J. Dutner, P. Mines, A. Anderson, Irrigation trends among American Association of Endodontists members: a web-based survey, J. Endod. 38 (2012) 37–40.

[16] K.A. Brogden, Antimicrobial peptides: pore formers or metabolic inhibitors in bacteria? Nat. Rev. Microbiol. 3 (2005) 238–350.

[17] D. Pletzer, R.E.W. Hancock, Antibiofilm peptides: potential as broad-spectrum agents, J. Bacteriol. 198 (2016) 2572–2578.

[18] D. Romeo, B. Skerlavaj, M. Bolognesi, R. Gennaro, Structure and bactericidal activity of an antibiotic dodecapeptide purified from bovine neutrophils, J. Biol. Chem. 263 (1988) 9573–9575.

[19] S.C. Mansour, C. de la Fuente-Núñez, R.E.W. Hancock, Peptide IDR-1018: modulating the immune system and targeting bacterial biofilms to treat antibiotic-resistant bacterial infections, J. Pept. Sci. 21 (2015) 323–329.

[20] T. Zhang, Z. Wang, R.E.W. Hancock, C. de la Fuente-Núñez, M. Haapasalo, Treatment of oral biofilms by a D-enantiomeric peptide, PLoS One 11 (2016) e0166997.

[21] D. Wang, Y. Shen, J. Ma, R.E.W. Hancock, M. Haapasalo, Antibiofilm effect of D-enantiomeric peptide alone and combined with EDTA in vitro, J. Endod. 43 (2017) 1862–1867.

[22] C. de la Fuente-Núñez, F. Reffuveille, E.F. Haney, S.K. Straus, R.E.W. Hancock, Broad-spectrum anti-biofilm peptide that targets a cellular stress response, PLoS Pathog. 10 (2014) e1004152.

[23] C. de la Fuente-Nunez, F. Reffuveille, S.C. Mansour, S.L. Reckseidler-Zenteno, D. Hernandez, G. Brackman, T. Coenye, R.E. Hancock, D-enantiomeric peptides that eradicate wild-type and multidrug-resistant biofilms and protect against lethal *Pseudomonas aeruginosa* infections, Chem. Biol. 22 (2015) 196–205.

[24] A. Kishen, A. Shrestha, A. Del Carpio-Perochena, Validation of biofilm assays to assess antibiofilm efficacy in instrumented root canals after syringe irrigation and sonic agitation, J. Endod. 44 (2018) 292–298.

[25] L. Lin, Y. Shen, M. Haapasalo, A comparative study of biofilm removal with hand, rotary nickel-titanium, and self-adjusting file instrumentation using a novel in vitro biofilm model, J. Endod. 39 (2013) 658–663.

[26] S. Bukhari, D. Kim, Y. Liu, B. Karabucak, H. Koo, Novel endodontic disinfection approach using catalytic nanoparticles, J. Endod. 44 (2018) 806–812.

[27] M. Ruiz-Linares, B. Aguado-Pérez, P. Baca, M.T. Arias-Moliz, C.M. Ferrer-Luque, Efficacy of antimicrobial solutions against polymicrobial root canal biofilm, Int. Endod. J. 50 (2017) 77–83.

[28] W.H. Ye, B. Fan, W. Purcell, M.M. Meghil, C.W. Cutler, B.E. Bergeron, J.Z. Ma, F.R. Tay, L.N. Niu, Anti-biofilm efficacy of root canal irrigants against in-situ *Enterococcus faecalis* biofilms in root canals, isthmuses and dentinal tubules, J. Dent. 79 (2018) 68–76.

[29] O.A. Peters, S. Bardsley, J. Fong, G. Pandher, E. DiVito, Disinfection of root canals with photon-initiated photoacoustic streaming, J. Endod. 37 (2011) 1008–1012.

[30] E.A. Bortoluzzi, D. Carlon Jr, M.M. Meghil, A.R. El-Awady, L. Niu, B.E. Bergeron, L. Susin, C.W. Cutler, D.H. Pashley, F.R. Tay, Efficacy of 3D conforming nickel titanium rotary instruments in eliminating canal wall bacteria from oval-shaped root canals, J. Dent. 43 (2015) 597–604.

[31] L.E. Chávez de Paz, J.R. Davies, G. Bergenholtz, G. Svensäter, Strains of *Enterococcus faecalis* differ in their ability to coexist in biofilms with other root canal bacteria, Int. Endod. J. 48 (2015) 916–925.

[32] R.D. Taylor, Modification of the Brown and Brenn gram stain for the differential staining of gram-positive and gram-negative bacteria in tissue sections, Am. J. Clin. Pathol. 461 (1966) 472–474.

[33] J.L. Hockett, J.K. Dommisch, J.D. Johnson, N. Cohenca, Antimicrobial efficacy of two irrigation techniques in tapered and non-tapered canal preparations: an in vitro study, J. Endod. 34 (2008) 1374–1377.

[34] M. Pourhajibagher, N. Chiniforush, S. Shahabi, R. Ghorbanzadeh, A. Bahador, Sub-lethal doses of photodynamic therapy affect biofilm formation ability and metabolic activity of *Enterococcus faecalis*, Photodiagnosis Photodyn. Ther. 15 (2016) 159–166.

[35] N. Zhang, K. Zhang, M.A. Melo, M.D. Weir, D.J. Xu, Y. Bai, H.H. Xu, Effects of long-term water-aging on novel anti-biofilm and protein-repellent dental composite, Int. J. Mol. Sci. 18 (2017) 186–200.

[36] L. Wang, X. Xie, S. Imazato, M.D. Weir, M.A. Reynolds, H.H. Xu, A protein-repellent and antibacterial nanocomposite for Class-V restorations to inhibit periodontitis-related pathogens, Mater. Sci. Eng. C Mater. Biol. Appl. 67 (2016) 702–710.

[37] P.N.R. Nair, On the causes of persistent apical periodontitis: a review, Int. Endod. J. 39 (2006) 249–281.

[38] R.N. Weller, S.P. Niemczyk, S. Kim, Incidence and position of the canal isthmus. Part 1. Mesiobuccal root of the maxillary first molar, J. Endod. 21 (1995) 380–383.

[39] Y.Y. Hsu, S. Kim, The resected root surface. The tissue of canal isthmuses, Dent. Clin. North Am. 41 (1997) 529–540.

[40] J.S. Webb, L.S. Thompson, S. James, T. Charlton, T. Tolker-Nielsen, B. Koch, M. Givskov, S. Kjellberg, Cell death in *Pseudomonas aeruginosa* biofilm development, J. Bacteriol. 185 (2003) 4585–4592.

[41] D. McDougald, S.A. Rice, N. Barraud, P.D. Steinberg, S. Kjelleberg, Should we stay or should we go: mechanisms and ecological consequences for biofilm dispersal, Nat. Rev. Microbiol. 28 (2011) 39–50.

[42] A. Mai-Prochnow, J.S. Webb, B.C. Ferrari, S. Kjelleberg, Ecological advantages of autolysis during the development and dispersal of *Pseudoalteromonas tunicata* biofilms, Appl. Environ. Microbiol. 72 (2006) 5414–5420.

[43] L. Hall-Stoodley, P. Stoodley, Biofilm formation and dispersal and the transmission of human pathogens, Trends Microbiol. 13 (2005) 7–10.

[44] E. O'Neill, C. Pozzi, P. Houston, H. Humphreys, D.A. Robinson, A. Loughman, T.J. Foster, J.P. O'Gara, A novel *Staphylococcus aureus* biofilm phenotype mediated by the fibronectin-binding proteins, FnBPA and FnBPB, J. Bacteriol. 190 (2008) 3835–3850.

[45] M.R. Kiedrowski, H.A. Crosby, F.J. Hernandez, C.L. Malone, J.O. McNamara 2nd, A.R. Horswill, *Staphylococcus aureus* Nuc2 is a functional, surface-attached extracellular nuclease, PLoS One 9 (2014) e95574.

[46] G. Donelli, I. Francolini, D. Romoli, E. Guaglianone, A. Piozzi, C. Ragunath, J.B. Kaplan, Synergistic activity of dispersin B and cefamandole nafate in inhibition of *staphylococcal* biofilm growth on polyurethanes, Antimicrob. Agents Chemother. 51 (2007) 2733–2740.

[47] I. Kolodkin-Gal, D. Romero, S. Cao, J. Clardy, R. Kolter, R. Losick, D-amino acids trigger biofilm disassembly, Science 328 (2010) 627–629.

[48] A. Peschel, M. Otto, Phenol-soluble modulins and staphylococcal infection, Nat. Rev. Microbiol. 11 (2013) 667–673.

[49] D. Wang, Y. Shen, R.E.W. Hancock, J. Ma, M. Haapasalo, Antimicrobial effect of peptide DJK-5 used alone or mixed with EDTA on mono- and multispecies biofilms in dentin canals, J. Endod. 44 (2018) 1709–1713.

[50] J.M. Parente, R.J. Loushine, L. Susin, L. Gu, S.W. Looney, R.N. Weller, D.H. Pashley, F.R. Tay, Root canal debridement using manual dynamic agitation or the EndoVac for final irrigation in a closed system and an open system, Int. Endod. J. 43 (2010) 1001–1102.

[51] L. Susin, Y. Liu, J.C. Yoon, J.M. Parente, R.J. Loushine, D. Ricucci, T. Bryan, R.N. Weller, D.H. Pashley, F.R. Tay, Canal and isthmus debridement efficacies of two irrigant agitation techniques in a closed system, Int. Endod. J. 43 (2010) 1077–1090.

[52] Z. Wang, C. de la Fuente-Núñez, Y. Shen, M. Haapasalo, R.E.W. Hancock, Treatment of oral multispecies biofilms by an anti-biofilm peptide, PLoS One 10 (2015) e0132512.

[53] A. Nijnik, L. Madera, S. Ma, M. Waldbrook, M.R. Elliott, D.M. Easton, M.L. Mayer, S.C. Mullaly, J. Kindrachuk, H. Jenssen, R.E. Hancock, Synthetic cationic peptide IDR-1002 provides protection against bacterial infections through chemokine induction and enhanced leukocyte recruitment, J. Immunol. 184 (2010) 2539–2550.

[54] H.B. Yu, A. Kielczewska, A. Rozek, S. Takenaka, Y. Li, L. Thorson, R.E. Hancock, M.M. Guarna, J.R. North, L.J. Foster, O. Donini, B.B. Finlay, Sequestosome-1/p62 is the key intracellular target of innate defense regulator peptide, J. Biol. Chem. 284 (2009) 36007–36011.

[55] P.G. Barlow, Y. Li, T.S. Wilkinson, D.M. Bowdish, Y.E. Lau, C. Cosseau, C. Haslett, A.J. Simpson, R.E. Hancock, D.J. Davidson, The human cationic host defense peptide LL-37 mediates contrasting effects on apoptotic pathways in different primary cells of the innate immune system, J. Leukoc. Biol. 80 (2006) (2006) 509–520.

[56] M.G. Scott, E. Dullaghan, N. Mookherjee, N. Glavas, M. Waldbrook, A. Thompson, A. Wang, K. Lee, S. Doria, P. Hamill, J.J. Yu, Y. Li, O. Donini, M.M. Guarna, B.B. Finlay, J.R. North, R.E. Hancock, An anti-infective peptide that selectively modulates the innate immune response, Nat. Biotechnol. 25 (2007) (2007) 465–472.

[57] M. Wieczorek, H. Jenssen, J. Kindrachuk, W.R. Scott, M. Elliott, K. Hilpert, J.Y. Cheng, R.E. Hancock, S.K. Straus, Structural studies of a peptide with immune modulating and direct anti-microbial activity, Chem. Biol. 24 (2010) 970–980.

[58] C. de la Fuente-Núñez, S.C. Mansour, Z. Wang, L. Jiang, E.B. Breidenstein, M. Elliott, F. Reffuveille, D.P. Speert, S.L. Reckseidler-Zenteno, Y. Shen, M. Haapasalo, R.E. Hancock, Anti-biofilm and immunomodulatory activities of peptides that inhibit biofilms formed by pathogens isolated from cystic fibrosis patients, Antibiotics (Basel) 3 (2014) 509–526.

[59] S.N. Kłodzińska, D. Pletzer, N. Rahanjam, T. Rades, R.E.W. Hancock, H.M. Nielsen, Hyaluronic acid-based nanogels improve in vivo compatibility of the anti-biofilm peptide DJK-5, Nanomedicine 3 (2019) 102022.

[60] M.R. Yeaman, N.Y. Yount, Mechanisms of antimicrobial peptide action and resistance, Pharmacol. Rev. 55 (2003) 27–55.

[61] A. Peschel, H.G. Sahl, The co-evolution of host cationic antimicrobial peptides and microbial resistance, Nat. Rev. Microbiol. 4 (2006) 529–536.

[62] B. Bechinger, S.U. Gorr, Antimicrobial peptides: mechanisms of action and resistance, J. Dent. Res. 96 (2017) 254–260.

[63] V. Hauryliuk, G.C. Atkinson, K.S. Murakami, T. Tenson, K. Gerdes, Recent functional insights into the role of (p)ppGpp in bacterial physiology, Nat. Rev. Microbiol. 13 (2015) 298–309.

[64] C.D. Fjell, J.A. Hiss, R.E.W. Hancock, G. Schneider, Designing antimicrobial peptides: form follows function, Nat. Rev. Drug Discov. 11 (2011) 37–51.

[65] A. Dehsorkhi, V. Castelletto, I.W. Hamley, Self-assembling amphiphilic peptides, J. Pept. Sci. 20 (2014) 453–467.

[66] Z. Ye, X. Zhu, S. Acosta, D. Kumar, T. Sang, C. Aparicio, Self-assembly dynamics and antimicrobial activity of all l- and d-amino acid enantiomers of a designer peptide, Nanoscale 11 (2018) 266–275.

[67] L. Schnaider, S. Brahmachari, N.W. Schmidt, B. Mensa, S. Shaham-Niv, D. Bychenko, L. Adler-Abramovich, L.J.W. Shimon, S. Kolusheva, W.F. DeGrado, E. Gazit, Self-assembling dipeptide antibacterial nanostructures with membrane disrupting activity, Nat. Commun. 8 (2017) 1365.

[68] M. Zhang, J. Zhao, J. Zheng, Molecular understanding of a potential functional link between antimicrobial and amyloid peptides, Soft Matter 10 (2014) 7425–7451.
[69] H. Hirt, J.W. Hall, E. Larson, S.U. Gorr, A D-enantiomer of the antimicrobial peptide GL13K evades antimicrobial resistance in the Gram-positive bacteria *Enterococcus faecalis* and *Streptococcus gordonii*, PLoS One 13 (2018) e0194900.
[70] M. Sieprawska-Lupa, P. Mydel, K. Krawczyk, K. Wójcik, M. Puklo, B. Lupa, P. Suder, J. Silberring, M. Reed, J. Pohl, W. Shafer, F. McAleese, T. Foster, J. Travis, J. Potempa, Degradation of human antimicrobial peptide LL-37 by *Staphylococcus aureus* derived proteinases, Antimicrob. Agents Chemother. 48 (2004) (2004) 4673–4679.
[71] J.C. Baumgartner, C.M. Brown, C.L. Mader, D.D. Peters, J.D. Shulman, A scanning electron microscopic evaluation of root canal debridement using saline, sodium hypochlorite, and citric acid, J. Endod. 10 (1984) 525–531.
[72] M. Zehnder, Root canal irrigants, J. Endod. 32 (2006) 389–398.
[73] G. Rossi-Fedele, E.J. Dogramaci, A.R. Guastalli, L. Steier, J.A. de Figueiredo, Antagonistic interactions between sodium hypochlorite, chlorhexidine, EDTA, and citric acid, J. Endod. 38 (2012) 426–431.
[74] M. Balić, R. Lucić, K. Mehadžić, I. Bago, I. Anić, S. Jakovljević, V. Plečko, The efficacy of photon-initiated photoacoustic streaming and sonic-activated irrigation combined with QMiX solution or sodium hypochlorite against intracanal *E. faecalis* biofilm, Lasers Med. Sci. 31 (2016) 335–342.
[75] A.K. Seth, M.R. Geringer, S.J. Hong, K.P. Leung, R.D. Galiano, T.A.A. Mustoe, Comparative analysis of single-species and polybacterial wound biofilms using a quantitative, in vivo, rabbit ear model, PLoS One 7 (2012) e42897.
[76] E.K. Manavathu, D.L. Vager, J.A. Vazquez, Development and antimicrobial susceptibility studies of in vitro monomicrobial and polymicrobial biofilm models with *Aspergillus fumigatus* and *Pseudomonas aeruginosa*, BMC Microbiol. 14 (2014) 53.
[77] Y.J. Yoo, H. Perinpanayagam, S. Oh, A.R. Kim, S.H. Han, K.Y. Kum, Endodontic biofilms: contemporary and future treatment options, Restor. Dent. Endod. 44 (2019) e7.